



EXPERIMENTAL SEISMIC PERFORMANCE OF NONSTRUCTURAL COMPONENTS FASTENED WITH DUCTILE ELEMENTS

T. Feinstein ⁽¹⁾, J. P. Moehle ⁽²⁾

⁽¹⁾ PhD Candidate, University of California Berkeley, talish@berkeley.edu

⁽²⁾ Professor, University of California Berkeley, moehle@berkeley.edu

Abstract

Damage of nonstructural components during an earthquake can impair the overall performance of a building through property damage, loss of functionality, and reduced occupant safety. Current Code provisions on the United States and elsewhere aim to minimize the threat to life safety by providing anchoring requirements for nonstructural components. These code requirements typically are based on a simplified equation that does not fully consider the contribution of the component attachment to the overall dynamic response of the component. Previous results from shaking-table tests of anchored components suggest that the component attachment is a key parameter that determines its dynamic properties. To evaluate this contribution, a nonstructural experimental model was attached to a concrete slab and tested on a shaking table with several attachment designs. The attachments were dimensioned based on a capacity design approach, such that they would be the weakest element in the force path while providing a yielding failure mechanism. The attachment designs provide different plastic mechanisms that control the displacement ductility in the response of the component. This paper focuses on the contribution of the attachment of the nonstructural component to the seismic force demand and the dynamic response. The experimental results suggest that the attachment properties govern the boundary conditions of the nonstructural component and that the use of attachments with increased ductility capacity does not necessarily result in reduced seismic loads.

Keywords: Earthquake Engineering, Nonstructural components, Shaking-table, Experimental earthquake simulation, Seismic performance.



1. Introduction

Nonstructural components have a major impact on structure recovery after an earthquake through repair costs, downtime and continued function of a structure. Financial losses from nonstructural components reach up to 80% of the damage costs after a seismic event [1]. Moreover, nonstructural damage could cause downtime of a structure even in cases where the structural system remains intact. Evaluation of anchored nonstructural components performance in recent earthquakes suggests that improvements in the design of the attachments of the component are required as many failures in anchorage and bracing systems have been observed [2].

Currently, nonstructural component design is focused on life safety and code provisions provide lateral force equations based on some simplifications and considering a few key parameters that are believed to provide an approximation of the dynamic force amplification of a nonstructural component [3]. Common parameters include the peak ground acceleration based on the seismic hazard, the nonstructural component location within the structure and some assumed nonstructural properties [4]. The practice of nonstructural seismic design usually allows only the design of the attachment, as the nonstructural component is a pre-designed manufactured product. There is little to no control over the design of the nonstructural component itself and commonly there is no information on the properties of it. Recent research on the seismic behavior of nonidealized nonstructural components suggests that the attachment of the component has a significant effect on the component acceleration and anchor forces and should be considered as key design parameters for the estimation of the lateral seismic load demand on the nonstructural components [5,6,7].

Recent research on improved seismic performance of nonstructural components presented a new approach to the design of nonstructural components oriented at defined performance objectives. Part of the research tackled the latest ASCE-7 lateral force equation and suggested a new version of the equation that replaced some of the simplifications in the equation with more advanced concepts based on information from instrumented structures [8]. In addition, the report includes general guidelines for the ductile design of supports and attachments of nonstructural components, suggesting that providing ductility in the load path between the component and the supporting structure through the angle connection would be an ideal requirement.

An experimental test program was developed to assess the contribution of the attachment design on the overall dynamic behavior of the nonstructural component. The design of the experimental model concentrated on the attachment design, based on both the importance of the attachment to the response and representing the main engineering feature that can be controlled by the engineer of record. An idealized nonstructural experimental model was designed to simulate a generic semi-rigid nonstructural component during the shaking-table tests. Two experimental models were constructed of steel and fitted with mass blocks on the top to mimic a single degree of freedom system. A concrete slab was placed on top of the shaking table to provide a realistic slab connection for the experiment and provide realistic boundary conditions. The experimental models were tested on a shaking-table attached using yielding angle connections with various plastic mechanisms. This paper describes the experimental setup and the influence of the attachment design on the dynamic response of the nonstructural component.

2. Experimental setup

The experimental setup was based on a Nonstructural Experimental Model (NEMO) that is representing a simplified 3-dimensional generic floor-anchored nonstructural component. The experiment focused on the contribution of designing a flexible attachment that provides ductility within the load path of the seismic loading. Thus, the NEMO was designed as a rigid component, constraining the deformation and nonlinear behavior into the attachment. The NEMO was designed with steel channels and angles to create a relatively



stiff box with a frequency of 18 Hz in the X direction and 15 Hz in the Y direction. The drawings and as made component are given in Fig.1. The NEMO's dimensions were 1.0m x 0.75m x 1.8m, and it was equipped with two 250 kg lead masses at the top of the component, resulting in the total weight of the NEMO was 700 kg. The design of the NEMO was chosen to closely resemble a single degree of freedom (SDOF) slender component that would be expected to exhibit rocking if it were to be free-standing. The NEMO was tested on the shaking-table attached to a concrete slab using instrumented post-installed anchors. The dynamic response of the NEMO was measured through accelerometers that were placed along the height of the component, at the bottom, center of gravity and top. Measurements also included displacement measurements from temposonics at the top to provide the total relative displacement, and at the bottom to record the slip and uplift of the base of the NEMO.

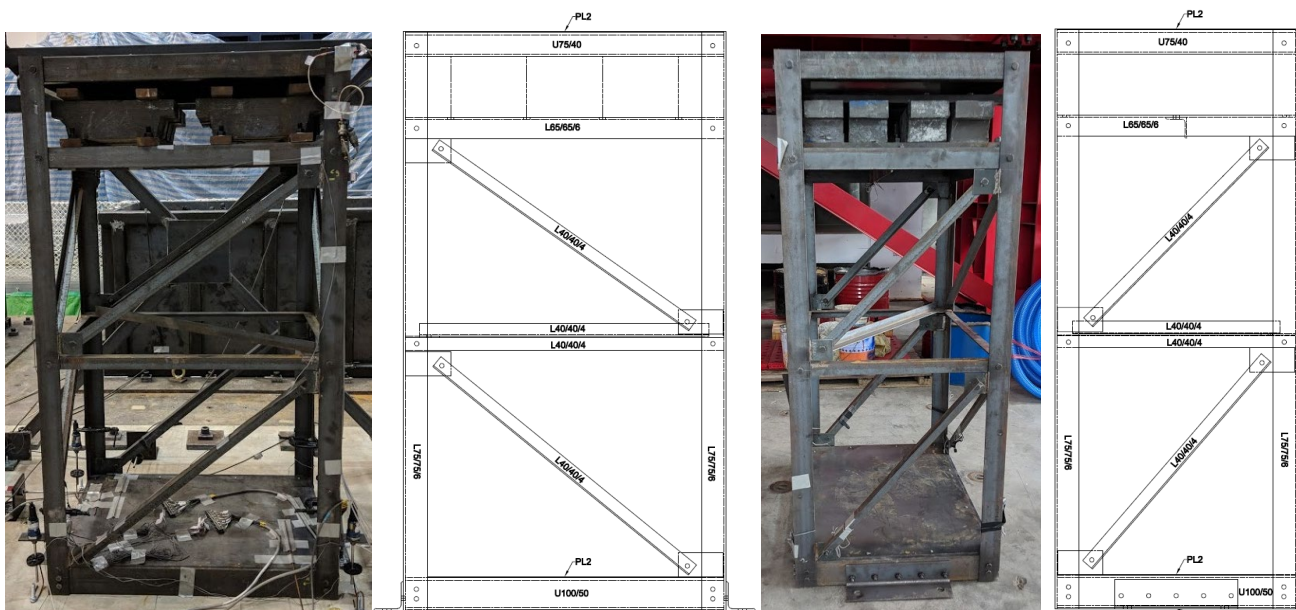


Fig.1 – Design of the NEMO (left) Strong axis – X (right) Weak axis – Y

The connection is based on two steel angles that are located at the bottom of the NEMO at two opposite sides on the X direction, as shown in Fig.1. The steel angles length is 380 mm with two different width options. The attachment was calculated according to capacity design principles and was designed to be weaker than the individual components of the NEMO, thus controlling the maximum force that would be transferred from the supports to the NEMO. The capacity design philosophy ensures that the yielding of the system would occur within the attachment, and provides an idealized system that focuses on the influence of the displacement ductility demand of the attachment while the component remains elastic. The steel angles were attached to the NEMO with 5 8.8 M12 bolts and attached to the concrete slab using 2 instrumented Hilti HSL-3-G M16 post-expansion anchors.

The experiment was developed to test the effects of different connection designs on the dynamic response of the nonstructural component. For this, four different designs of connections were tested, varying in capacity and allowable plastic hinge length. The four designs were divided into two pairs of angles made from the same thickness angles, with two different geometries that differ by the distance from the angle base to the anchor location, as illustrated in the drawing in Fig.2. Both angles provide the same moment capacity, but have a different yielding mechanism, with the longer geometry allowing for a larger angle to form with a larger plastic hinge length, resulting in a larger ductility capacity of the angles with the longer geometry.



Each pair of angles was tested simultaneously on the shaking-table with two different NEMOs to allow the direct comparison between the two different yielding mechanisms that are illustrated in Fig.3 with low flexibility in (a) and large flexibility in (b). Angles (a) and (b) in Fig.2 are referred to as the thick angles and were made of 7 mm hot-rolled steel. Angles (c) and (d) in Fig.2 are referred to as the thin angles and were made of 2.3 mm cold-rolled steel. The difference in thickness provided two sets of angles with varying moment capacity, such that it provided two different force limits of the attachment.

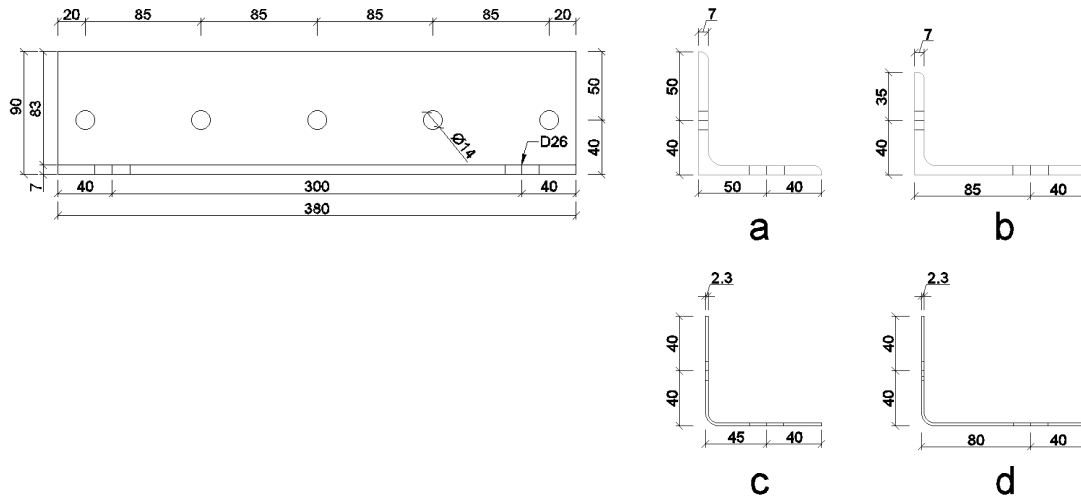


Fig.2 - Design of the thick pair of steel angles for the NEMO's connection (a) Thick-Short (b) Thick-Long (c) Thin-Short (d) Thin-Long

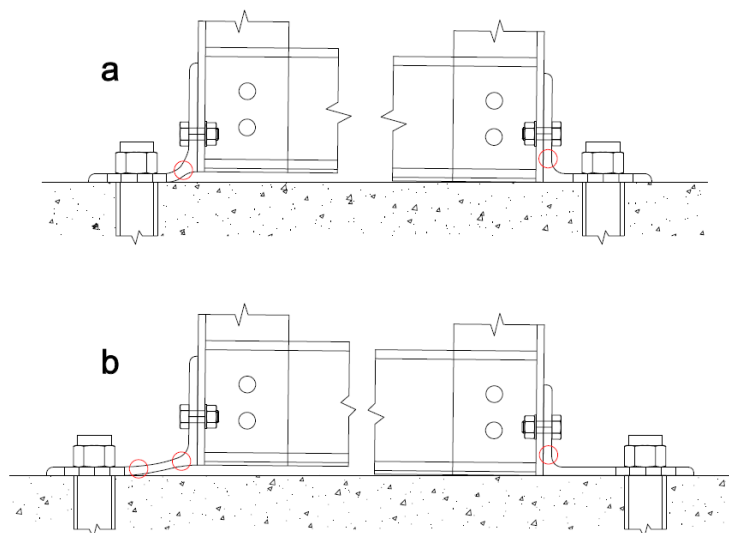


Fig.3 - Angle deformed shapes due to component uplift with plastic hinge locations. (a) Thick-Short angles (b) Thick-Long angles



3. Input Motions

The input motions that were chosen for the test were recorded near-fault ground motions with a Peak Ground Acceleration (PGA) of 0.8g. The ground motion selection was based on a velocity pulse identification algorithm [9] to create the basis of eight ground motions for the test program. The response spectra of the ground motions that were chosen are given in Fig.4 for the three principal directions of motion. The loading protocol for each ground motion included six variations that are listed in Table 1 with the scaling of the original recording in each direction, two additional runs with an input of white noise were performed before the 100% motions and at the end of the sequence.

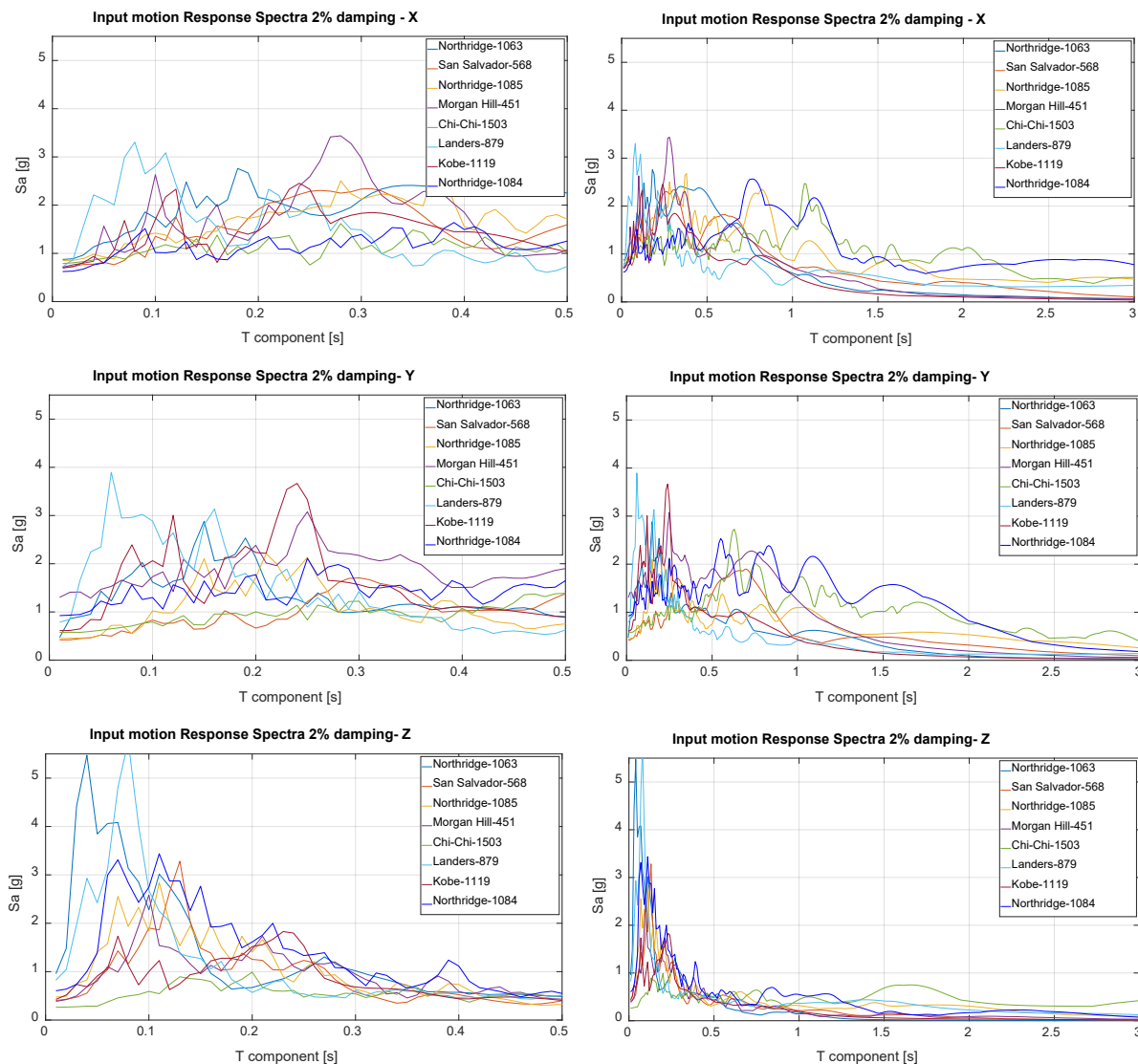


Fig.4 - Input motion spectra for the three direction of input motion.



Traditionally nonstructural components are designed based on the PGA, as their natural periods are considerably short. However, when the nonstructural component is not restricted from uplifting it can result in a longer period response that could be amplified from long period pulses. Near-fault motions might contain large pulse-like motions at longer periods and might affect nonstructural components that exhibit partial rocking response.

Table 1 – Loading protocol for each recording

| Run number | X-Direction [%] | Y-Direction [%] | Z-Direction [%] |
|------------|-----------------|-----------------|-----------------|
| 1 | 50.0 | 0.0 | 0.0 |
| 2 | 0.0 | 50.0 | 0.0 |
| 3 | 100.0 | 0.0 | 0.0 |
| 4 | 0.0 | 100.0 | 0.0 |
| 5 | 100.0 | 100.0 | 0.0 |
| 6 | 100.0 | 100.0 | 100.0 |

4. Results

The influence of the connection design on the nonstructural component dynamic response was studied during the test program. The different connections provided different yielding mechanisms and capacities that transformed the response of the NEMO to seismic loading. The dynamic response of the NEMO was quantified through the measured accelerations and displacements during the shaking-table tests. The response was evaluated through three observations, the first was the shifts of the first natural period of the NEMO, the second included the amplification of the NEMO acceleration compared to the input table acceleration, and the last focused on the displacement modes of the NEMO.

4.1. Natural Period

The natural period of the NEMO was estimated based on the response of the NEMO to shaking-table tests with white noise input motion. The first natural period was determined based on the largest amplitude of the acceleration response of the NEMO after transformation to the frequency domain. White noise tests were performed after the 50% scaled motion of each recording and at the end of all the runs of each recording. The natural frequency from all the white noise tests for each of the connection design of the NEMO is given in Fig.5 and shows that for the most part, the natural frequencies are constant throughout the test program. These constant frequencies were transformed into natural periods and are summarized in Table 2.

There is a large variation in natural periods between the various connection designs of the NEMOs that is observed in Fig.5 and the average values in Table 2. This large variation demonstrates the importance of the connection design on the basic properties of the nonstructural element overall system, with results that show that the same nonstructural component can have a natural period that varies from a 0.06 sec to 0.5 sec. The smallest natural period, observed for the thick-short connection design, was lower than 0.06 seconds, which is considered as a rigid component according to the AC156 guidelines [10]. In contrast, the thin-long connection design resulted in a very flexible system response, with a natural frequency of about 0.5 seconds.



A comparison between the same thickness connections with different geometries suggests that changing the geometry of the connection and adding flexibility while maintaining the same moment capacity has a significant effect on the dynamic response of the overall system. A 60% change in the natural frequency in the Y direction can be observed in Fig.5 between the thick angles with the long and short geometry, and a 30% change in the X direction for the same pair of connections. The thin pair of connections have shown a less significant change of 20% in both principal directions.

Table 2 – Effects of the connection on the component natural period

| Connection | Period - X direction [s] | Period - Y direction [s] |
|---------------|--------------------------|--------------------------|
| Thick – Short | 0.057 | 0.098 |
| Thick – Long | 0.074 | 0.247 |
| Thin – Short | 0.158 | 0.434 |
| Thin – Long | 0.189 | 0.513 |

The changes in the natural period between the different designs of connection point at the significant role of the attachment of the nonstructural component in the dynamic properties of the overall system of the nonstructural component. The change of the length between the NEMO and the anchor location has caused a change in the boundary conditions of the connection of the NEMO to the slab and caused a significant change in the period of the response of the NEMO.

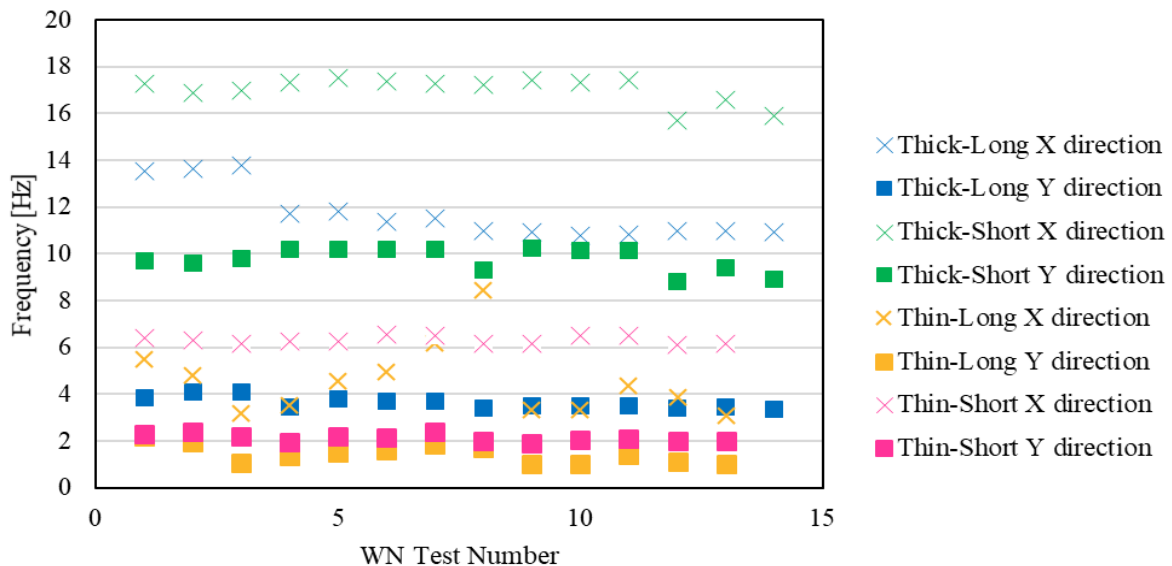


Fig.5 – NEMO 1st natural frequency based on White Noise input motion tests



4.2. Component Amplification

Floor-mounted nonstructural components are considered mostly as acceleration sensitive elements. The Peak Component Acceleration (PCA) of the NEMO was determined as the peak acceleration that was measured at the center of gravity of the NEMO during each test, based on the average of two accelerometers at the center of gravity height. The PCA was then normalized based on the Peak Floor Acceleration (PFA) that was measured on the concrete slab for the same input motion. The component amplification is measured as the normalized value of PCA/PFA for a specific test. The component amplification was calculated for each principal direction separately and is presented for all the tests in Fig.6 in two different colors, separated into two plots according to the connection thickness. The two NEMOs with different connection geometries that were tested simultaneously on the shaking-table are represented as triangles for the short geometry and circles for the long geometry.

The range of component amplification that can be observed in Fig.6 has a maximum of 5.4 and a minimum of 0.5, which fits the response spectra for the input motions that were used during the test plan and are given in Fig.4. A comparison between the two plots reveals that the component amplifications with the thin connections are in a lower range than with the thick connections. The main reason for the improved behavior of the thin anchor can be associated with the elongated natural period of the NEMO; in the Y direction the natural period is about 0.5 seconds for the thin connections, which for the recorded motion from the Landers earthquake results in de-amplification of the response, as can be seen in Fig.4 in the light blue response spectrum.

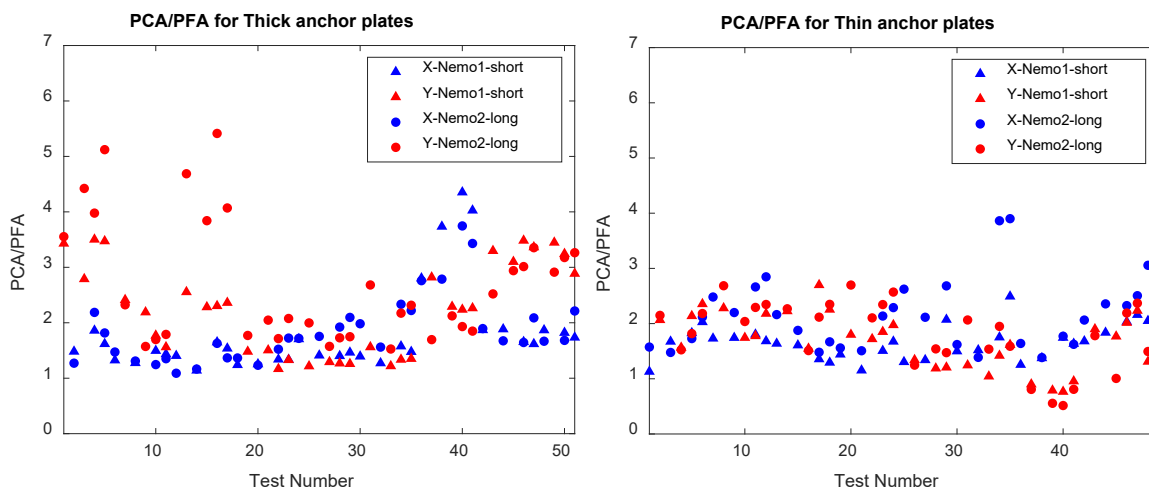


Fig.6 - Acceleration amplification factors, (left) Thick angle connections, (right) Thin angle connections.

Comparison of the two NEMOs that were tested simultaneously, with the long angle geometry and the short angle geometry brings to light interesting observations. The higher ductility capacity that was provided with the longer geometry did add flexibility and increased the displacements. However, the long angle design has performed relatively poorly compared to the same thickness short design, resulting in higher component amplification in 70% of the 153 shaking-table tests that were performed.



4.3. Rigid Body Rotation

The dynamic response of the NEMO can be separated into two modes of behavior, one is the flexible displacement and the second is rigid body rotation. The contribution of each of the modes to the total displacement response was calculated based on the displacement measurements. The top displacement that has originated from rigid body rotation has been calculated from the base rotation that was measured through 4 temposonics that were placed at the base corners of the NEMO and measured the uplift. An example of the uplift caused by the rigid body rotation of the NEMO is presented in Fig.7, showing the base of the NEMO attached with the thin-long angles uplifting during the Morgan Hill input motion.



Fig.7. Uplift of NEMO attached with the long-thin angles during Morgan Hill motion.

The contribution of each mode of response was compared between the different connection designs based on the top relative displacement history of the NEMOs for the same input motion. An example of the comparison is given in Fig.8, with the total top relative displacement and the contribution of the rigid body rotation for the recorded motion from Landers earthquake. It can be observed that the contribution of the rigid body rotation varies between the different connection designs, with a clear distinction that as the flexibility grows the rigid body rotation contributes more to the displacement response. The 4 different connection designs provide a wide range of responses, with the contribution of the rigid body rotation to the total relative top displacement response of the NEMO varying from 10% for the thick-short connection, through 20% for the thick-short connection, 67% for the thin-short connection and almost the entire displacement response for the thin-long connections. These results emphasize the importance of the connection design of nonstructural components, as it demonstrates that different connection design can significantly change the response of a nonstructural component.

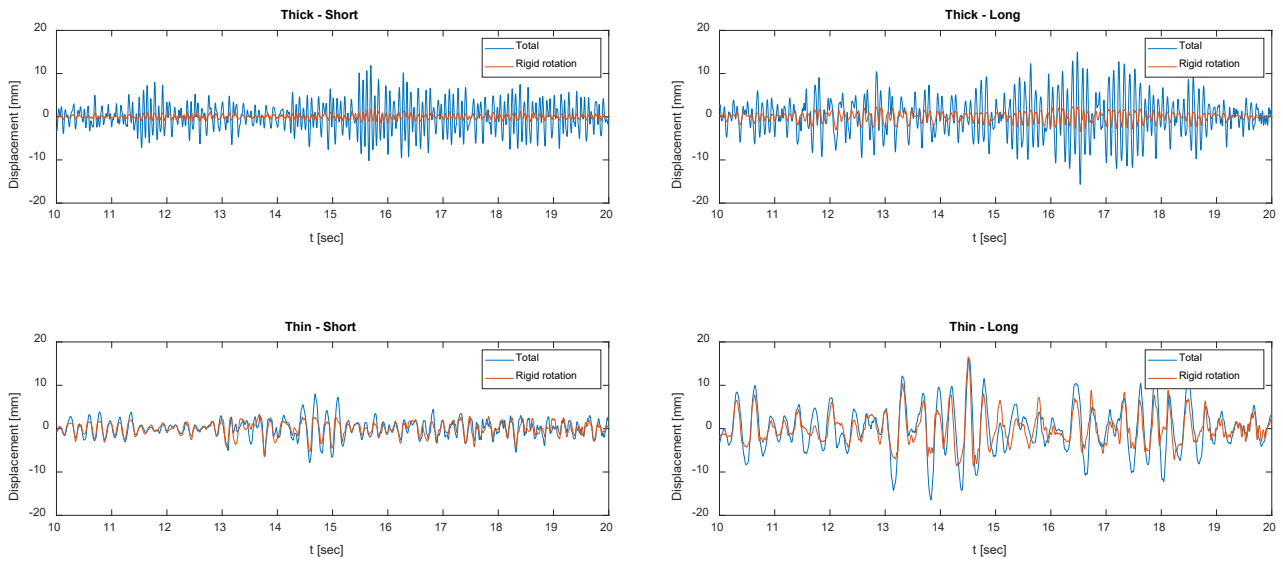


Fig.8 - Total top displacement of the NEMO compared to the top displacement contribution only from rigid body rotation for Landers recorded motion.

5. Conclusions

An experimental test program was developed to assess the contribution of the attachment design on the overall dynamic behavior of a floor-mounted nonstructural component. An idealized nonstructural component was tested on a shaking table attached with angle connections with various plastic mechanisms. The performance of the NEMO with the different connections was evaluated with eight recorded near-fault ground motions. The results from the experiments confirm the main role of the connection in the dynamic response of the nonstructural component.

Different attachment design of a nonstructural component has a significant impact on the dynamic properties of the overall system, which can be observed with shifting of the natural period of the response of the system. In this test program, a change of 500% in the natural period was observed between the shortest period and the longest period of the NEMO with different attachments.

The nonstructural component response during the experiment has shown that the dynamic behavior is controlled by two mechanisms including rigid body rotation and the flexible response of the component. The contribution of each of the two mechanisms to the total response is controlled by the flexibility and yielding mechanism of the attachment. The four attachment designs included a wide range of responses and suggest that additional ductility through changing the plastic hinge mechanism in the attachment of a nonstructural component can cause an amplified response of the nonstructural component. The change in the yielding mechanisms permits uplift displacements at the bottom of the nonstructural component and changes the response to a rigid body motion rather than flexible fixed base behavior.



6. Acknowledgments

The presented test program has been done through a joint project with the National Center for Research on Earthquake Engineering (NCREE) in Taiwan. The assistance provided by NCREE throughout the design process of the experiment and execution, and the support given by the shaking-table staff at NARlabs in Tainan, were essential to the success of the test program. In addition, the technical advice and professional perspective given by Hilti corporation and Estructure have been a crucial help in the design of the experiment.

7. References

- [1] Taghavi S. and Miranda E. (2003). Response assessment of nonstructural building elements, *Pacific Earthquake Engineering Research Center*, **5**.
- [2] Miranda E, Mosqueda G, Retamales R and Pekcan G. (2012). Performance of Nonstructural Components during the 27 February 2010 Chile Earthquake. *Earthquake Spectra*, **28** (1): 453-471.
- [3] ASCE/SEI-7-16 (2017). Minimum design loads for buildings and other structures, *American Society of Civil Engineers*, Reston, VA.
- [4] Johnson T.P., Dowell R.K. and Silva J.F. (2016). A review of code seismic demands for anchorage of nonstructural components, *J. of Building Engineering*, **5**, 249-253.
- [5] Feinstein T, Mahin S. (2018). Experimental Performance of Floor Mounted Nonstructural Components Under Seismic Loading. *Proceedings of the 11th National Conference in Earthquake Engineering, Earthquake Engineering Research Institute*, Los Angeles, CA, USA.
- [6] Feinstein T, Mahin S. (2018). Shake Table Tests to Evaluate Seismic Performance of Floor Mounted Nonstructural Components. *Proceedings of the 16th European Conference on Earthquake Engineering*, Thessaloniki, Greece.
- [7] Feinstein T, Moehle J.P., Mahin S.A. (2018). Anchored nonstructural component response to seismic loading - shaking table tests report. *Pacific Earthquake Engineering Research (PEER) Center, University of California, Berkeley, SEMM*, **5**.
- [8] ATC (2018). Recommendations for Improved Seismic Performance of Nonstructural Components, *NIST*, CA, USA.
- [9] Shahi, S.K. and Baker, J.W. (2014). "An efficient algorithm to identify strong velocity pulses in multi-component ground motions." *Bulletin of the Seismological Society of America*, 104(5), 2456–2466.
- [10] AC156 (2010). Acceptance Criteria for Seismic Certification by Shake-Table Testing of Nonstructural Components, International Code Council.